

# **Photocatalytic Degradation of Reactive Black 5 Dye by using commercial TiO<sub>2</sub> nanopowder and synthesised TiO<sub>2</sub> nanotubes**

Dissertation submitted in partial fulfillment for the requirement of degree of

**Master of Technology  
in  
Environmental Science and Technology**

**By:**

**Veni Mittal**

(Roll No. 601101027)

Under the supervision of

Dr. Pramod K. Bajpai  
Distinguished Professor  
Department of Chemical Engineering

Dr. Haripada Bhunia  
Associate Professor  
Department of Chemical Engineering



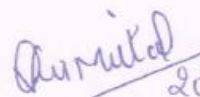
**SCHOOL OF ENERGY AND ENVIRONMENT  
THAPAR UNIVERSITY  
PATIALA-147004**

**June 2013**

## CERTIFICATE

This is to certify that the dissertation entitled "**Photocatalytic degradation of Reactive Black 5 dye by using commercial TiO<sub>2</sub> nanopowder and synthesized TiO<sub>2</sub> nanotubes**" is an authentic record of my own work carried out as requirements for the award of degree of Master of Technology in Environmental Science & Technology from Thapar University, Patiala, under the guidance of Dr. Pramod K. Bajpai (Distinguished Professor, ChED) and Dr. Haripada Bhunia (Associate Professor, ChED) during June 2012 to June 2013.

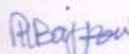
Date: 20/6/13.


  
20<sup>th</sup> June 13.

Veni Mittal


(Roll No: 601101027)

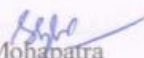
It is certified that the above statement made by the student is correct to the best of our knowledge and belief.

  
Dr. P. K. Bajpai  
Distinguished Professor  
Department of Chemical Engineering  
Thapar University, Patiala

  
Dr. Haripada Bhunia  
Associate Professor  
Department of Chemical Engineering  
Thapar University, Patiala

### Countersigned by

  
Dr. A. S. Reddy  
Head, School of Energy and Environment  
Thapar University, Patiala

  
Dr. S. K. Mohapatra  
Dean of Academic Affairs  
Thapar University, Patiala

## ACKNOWLEDGEMENTS

I express my sincere gratitude and regards to my supervisor Dr. Pramod K. Bajpai, Distinguished Professor, Department of Chemical Engineering, Thapar University, Patiala for his valuable guidance and suggestions. Without his encouragement and guidance this thesis would not have been materialized.

I feel privileged to offer my sincere thanks and owe an enormous deal of gratitude to my co-supervisor Dr. Haripada Bhunia, Associate Professor, Department of Chemical Engineering, Thapar University Patiala, for his guidance and encouragement at every step of my work.

I would like to express my gratitude to Dr. A. S. Reddy, Head of School of Energy and Environment Thapar University, Patiala for his kind cooperation and encouragement which helped in the completion of this work.

I would like to thank Dr. Rajeev Mehta, Head of Chemical Engineering Department, Thapar University, Patiala for supporting me and providing an environment to complete my work successfully.

I would like to thank Technical Education Quality Improvement Programme (TEQIP) Phase-II, Thapar University for financial support in presenting the published papers

I would like to thank Dr. Sandeep Sharma, Chitrakshi Goel(Inspire fellow), Kimi Jain(Research scholar) an Gaurav Madhu(Research Associate) for their constant help and support at various stages of my work.

Above all, I express my indebtedness to the “**ALMIGHTY**” for all His blessing and kindness.

Veni Mittal

(Roll No:  
601101027)

## ABSTRACT

The textile industries use a number of dyes, chemicals to impart desired quality to the fabrics. These industries generate a substantial quantity of effluents which cause environmental problems, if disposed off without proper treatment. At present, due to the increasing resource constraints and the environmental requirements, these textile industries need to adopt a sustainable approach, and wastes generated therefore to be viewed as unutilized resources. Ways and means must be found to recover water and chemicals from these “waste” resources. The conventional treatment processes have various disadvantages and limitations, therefore, cannot be successfully implemented in the textile industry. Advanced oxidation processes seem to be promising as these methods can efficiently degrade the highly toxic and recalcitrant compounds and do not generate any secondary pollutants for disposal.

Heterogeneous photocatalysis is the promising method among AOP's to remove colorants and also to completely degrade into simple substances like CO<sub>2</sub>, H<sub>2</sub>O and mineral acids. Various catalysts are used of which one of the most is studied TiO<sub>2</sub> due to its unique features such as absolute and relative band positions. The main disadvantage of using TiO<sub>2</sub> is the recombination of electrons and holes which can decrease the efficiency of the process which can be overcome by modifying its structure or incorporating some impurities.

This thesis seeks to give a method to study the kinetics of adsorption and of photocatalytic degradation of bare TiO<sub>2</sub> as well as TiO<sub>2</sub> nanotubes . The dye used was Reactive black 5.

The **1<sup>st</sup> chapter** is an introduction, giving an overview of the situation and of the photocatalytic process

The **2<sup>nd</sup> chapter** is the literature review

The **3<sup>rd</sup> chapter** describes the materials and methods used during this research work.

The **4<sup>th</sup> chapter** is the results and discussion which includes kinetics and photocatalytic activity of bare TiO<sub>2</sub> and TiO<sub>2</sub> nanotubes.

The **5<sup>th</sup> chapter** includes conclusion

The **6<sup>th</sup> chapter** includes recommendations and future work

# CONTENTS

<b>Title</b>	<b>Page No.</b>
Certificate	i
Acknowledgment	ii
Abstract	iii
Contents	iv
List of figures	vi
List of tables	viii
Abbreviations	ix
Chemical formulae	xi
<b>Chapter 1 Introduction</b>	<b>1-8</b>
1.1 Categorization of waste generated in textile industry	2
1.1.1 Hard to treat waste	3
1.1.2 Hazardous or toxic waste	3
1.1.3 High volume waste	4
1.1.4 Dispersible waste	4
1.2 Advanced Oxidation process	
5	
<b>Chapter 2 Literature Review</b>	<b>9-13</b>
2.1 Generalities	9
2.2 Heterogeneous Catalysts	9
2.3 Modified TiO <sub>2</sub>	10
<b>Chapter 3 Materials and Methods</b>	<b>14-18</b>
3.1 Materials	14
3.1.1 Chemicals and reagents	14
3.1.2 Catalyst	14
3.2 Instruments	15
3.2.1 Radiometer	15
3.2.2 pH meter	15
3.2.3 UV-Vis spectrophotometer	15

	3.2.4 Centrifuge	15
	3.2.5 Photoreactor	15
	3.3 Experimental procedures	17
	3.3.1 Method for preparation of TiO <sub>2</sub> nanotubes	17
	3.3.2 Optimization of parameters	17
	3.3.3 Photocatalytic Treatment	17
<b>Chapter 4</b>	<b>Results and Discussion</b>	<b>19-28</b>
	4.1 Kinetics of adsorption	19
	4.1.1 Kinetics of bare TiO <sub>2</sub>	19
	4.2 Adsorption isotherms	20
	4.3 Thermodynamic parameters	
23		
	4.4 Photocatalytic degradation studies	23
	4.5 Adsorption on TiO <sub>2</sub> nanotubes	25
	4.6 Photocatalytic degradation studies	25
	4.7 Recycling of TiO <sub>2</sub> nanotubes	26
	4.8 Effect of pH	28
<b>Chapter 5</b>	<b>Conclusion</b>	<b>29</b>
<b>Chapter 6</b>	<b>Recommendation and Future work</b>	<b>30</b>
	<b>References</b>	<b>31-34</b>
	<b>Publication</b>	<b>35</b>

## LIST OF FIGURES

<b>Fig</b>	<b>Description</b>	<b>Page No.</b>
1.1	Schematic representation of wastewater treatment plant	4
1.2	TiO <sub>2</sub> -semiconductor photocatalytic process. Scheme showing some photochemical and photophysical events that might take place on an irradiated semiconductor particle	5
3.1	Structure of Reactive black 5	14
3.2	Scheme of the photocatalytic reactor	16
3.3	Photograph of the photocatalytic reactor set up	16
3.4	TiO <sub>2</sub> nanotubes setup	18
4.1	Adsorption studies of RB 5 by TiO <sub>2</sub> (Dye conc. =50 mg/l, pH=4)	19
4.2	Adsorption isotherm of RB 5 onto TiO <sub>2</sub> surface (Dye conc. =50 mg/l, pH=4)	21
4.3	Langmuir adsorption isotherm of RB 5 onto TiO <sub>2</sub> surface (Dye conc. = 50 mg/l, pH=4)	21
4.4	Freundlich adsorption isotherm of RB 5 into TiO <sub>2</sub> surface (Dye conc. = 50 mg/l, pH=4)	22
4.5	Photodegradation of RB 5 on TiO <sub>2</sub> surface (Dye conc. = 200 mg/l, cat load= 2.0 g/l, pH=4)	24
4.6	Adsorption studies of RB 5 by TiO <sub>2</sub> nanotubes (Dye conc. = 50 mg/l, pH=2)	24
4.7	Photoderadation of RB 5 by TiO <sub>2</sub> nanotubes (Dye conc. = 200 mg/l, cat load= 2.0 g/l, pH=2)	25
4.8	RB5 degradation for the recycling experiments of the bare TiO <sub>2</sub> and TiO <sub>2</sub> nanotubes	27

## LIST OF TABLES

Table No.	Description	Page
1.1.	Typical characteristics of textile effluent	2
3.1	Physiochemical properties of Degussa P25 TiO <sub>2</sub>	15
4.1	Adsorption kinetic parameters for different catalyst load (0.125 g/l-1.75.0 g/l) for 50 mg/l dye concentration at pH=4	20
4.2	Langmuir and Freundlich isotherm for adsorption of RB 5 on TiO <sub>2</sub> surface (Dye conc. =50mg/l, pH=4)	22
4.3	Thermodynamic parameters of the adsorption of RB 5 on TiO <sub>2</sub> surface ( Dye conc. =50 mg/l, pH=4)	23

## ABBREVIATIONS

AOX	Adsorbable organic halogen
AOP	Advanced oxidation process
AR	Analytical reagent
BET	Branauer-Emmett-Teller
BOD	Biochemical oxygen demand
CB	Conduction band
COD	Chemical oxygen demand
$e^-$	Electron
ev	electron volt
g	gram
g/l	gram per litre
$h^+$	Hole
h	Plancks constant
l/mg	Litres per milligram
Ltd.	Limited
LI	Liquid impregnation
mg	Milligrams
mg/g	Milligrams per gram
mol	moles
nm	Nanometer
no.	Number
PEG	Polyethylene glycol
ppm	Parts per million
pvt.	Private
RPM	Revolutions per minute
RB 5	Reactive Black 5
TOC	Total organic carbon
UNESCO Organisation	United Nations Educational, Scientific and Cultural
UNICEF	United Nations Children's Fund
US	Ultrasound
UV	Ultraviolet

WHO	World Health Organization
VB	Valence band
Vis	Visible
ZPC	Zero point charge

## CHEMICAL FORMULAE

$\text{TiO}_2$	Titanium dioxide
$\text{H}_2\text{O}_2$	Hydrogen peroxide
$\text{O}_3$	Ozone
$\text{OH}\bullet$	Hydroxyl radical
$\text{O}_2^-\bullet$	Superperoxide radical
$\text{CO}_2$	Carbon dioxide
$\text{H}_2\text{O}$	Water
$\text{KMnO}_4$	Potassium permanganate
$\text{O}_2$	Dioxygen
$\text{ZnO}$	Zinc oxide
$\text{WO}_3$	Tungsten oxide
$\text{MVO}_4$	Metal vanadates
$\text{In}_2\text{O}_3$	Indium oxide
$\text{CeO}_2$	Cerium oxide
$\text{AgNO}_3$	Silver nitrate
$\text{HCl}$	Hydrochloric acid
$\text{NaOH}$	Sodium hydroxide

# CHAPTER 1

## INTRODUCTION

Water is a pre-requisite for life and an adequate water supply in both quantity and quality is necessary for human existence. Water covers 3 quarters of the earth surface but only 2.5 % is non salty. Out of this 2.5 % world's fresh water less than 1 % is readily available for human use and is unevenly distributed [1]. World water consumption per year is about  $10^4 \text{ km}^3$  and, at present, the quantity of available potential drinking water per year is between 10 and  $30 \times 10^3 \text{ km}^3$  [2]. Therefore, even a small shortage of water could become a threat to mankind.

Our biosphere is under regular threat from continuing environmental pollution. Its impact on atmosphere, hydrosphere and lithosphere by anthropogenic activities can't be ignored. Activities on water by domestic, industrial, agriculture, radio-active, aquaculture wastes; on air by industrial pollutants, mobile combustion, burning of fuels, agricultural activities, ionization radiation, cosmic radiation, suspended particulate matter; and on land by domestic wastes, industrial waste, agricultural chemicals and fertilizers, acid rain, animal waste have generated negative influence over biotic and abiotic components on different natural ecosystems. Most serious threat is the addition of non-biodegradable and toxic compounds in the ecosystem leading to the degradation of the quality of water sources and therefore of the drinking water.

Among all the disciplines of engineering, Textile Engineering has a direct connection with environmental aspects to be abundantly considered. The main reason is that the textile industry plays an important role in the economy of the country like India and it accounts for around one third of total export. Out of various activities in textile industry, chemical processing contributes about 70% of pollution. Typical characteristics of textile effluent are shown in **Table 1.1**.

It is very well known that cotton mills consume large volume of water for many processes such as sizing, scouring, bleaching, dyeing, printing, finishing and ultimately washing. Due to the nature of various chemical processing of textiles, large volumes of waste water with numerous pollutants are discharged. Thus, a study on many measures which can be adopted to treat the waste water discharged from textile chemical processing industries to protect and safeguard our surroundings from possible pollution problem has been the focus point of many recent investigations. The wastewater released from the textile industry is solution of complex chemical with high colour value. The colour in the effluent is mainly due to unfixed

dye. The concentration of unused dyes in the effluent depends upon the nature of dyes and dyeing process underway at the time. The treatments commonly used by the textile industries to treat their wastewaters are diverse. They are usually separated in preliminary, primary, secondary and tertiary stage. The preliminary treatment removes debris and sandy materials usually by a screening process. The primary treatment is the second step in separating undissolved materials. It removes suspended solids and greases from wastewater.

The processes used in this treatment are physical: screening, sedimentation, flocculation, flotation. The secondary treatment is a biological treatment with micro-organisms. It is used to remove dissolved organic matter from the wastewater. The micro-organisms absorb organic matter from sewage as their food supply. The tertiary stage also called advanced wastewater treatment is usually used to achieve high quality effluent discharge.

It focuses on the removal of nutrient, phosphorus and solids. Dissolved solid removal for example can involve ion exchange, micro-porous membrane filtration, nano-filtration, reverse osmosis, adsorption and chemical oxidation [3].

**Table 1.1.** Typical characteristics of textile effluent [4]

pH	6.0-10.0
Temperature	35-45 <sup>0</sup> C
BOD (mg/l)	100-4000
COD (mg/l)	150-10,000
Total Suspended Solids (mg/l)	100-5000
Total Dissolved Solids (mg/l)	1800-6000
Chlorides (mg/l)	1000-6000
Total Alkalinity (mg/l)	500-800
Sodium (mg/l)	600-2175
Total Kjeldahl Nitrogen (mg/l)	70-80
Color (Pt-Co units)	50-2500

### 1.1 Categorization of Waste Generated in Textile Industry

Textile waste is broadly classified into four categories, each of having characteristics that demand different pollution prevention and treatment approaches. Such categories are discussed in the following sections:

### **1.1.1 *Hard to Treat Wastes***

This category of waste consists of those that are persistent, resist treatment, or interfere with the operation of waste treatment facilities. Non-biodegradable organic or inorganic materials are the chief sources of wastes, which contain colour, metals, phenols, certain surfactants, toxic organic compounds, pesticides and phosphates. The chief sources [5] are

- Colour & metal -dyeing operation
- Phosphates - preparatory processes and dyeing
- Non-biodegradable organic materials - surfactants

Since these types of textile wastes are difficult to treat, the identification and elimination of their sources are the best possible ways to tackle the problem. Some of the methods of prevention are chemical or process substitution, process control and optimization, recycle/reuse and better work practices.

### **1.1.2. *Hazardous or Toxic Wastes***

These wastes are a subgroup of hard to treat wastes. But, owing to their substantial impact on the environment, they are treated as a separate class. In textiles, hazardous or toxic wastes include metals, chlorinated solvents, non-biodegradable or volatile organic materials. Some of these materials often are used for non-process applications such as machine cleaning.

### **1.1.3. *High Volume Wastes***

Large volume of wastes is sometimes a problem for the textile processing units. Most common large volume wastes include:

- High volume of waste water
- Wash water from preparation and continuous dyeing processes and alkaline wastes from preparatory processes
- Batch dye waste containing large amounts of salt, acid or alkali

These wastes sometimes can be reduced by recycle or reuse as well as by process and equipment modification.

#### 1.1.4. Dispersible Wastes:

The following operations in textile industry generate highly dispersible waste:

- Waste stream from continuous operation (e.g. preparatory, dyeing, printing and finishing)
- Print paste (printing screen, squeeze and drum cleaning)
- Lint (preparatory, dyeing and washing operations)
- Foam from coating operations
- Solvents from machine cleaning
- Still bottoms from solvent recovery (dry cleaning operation)

A major class of all colorants used worldwide is represented by azo dyes such as (1) comprising of azo link(s) flanked by substituted aromatic or heterocyclic moieties.

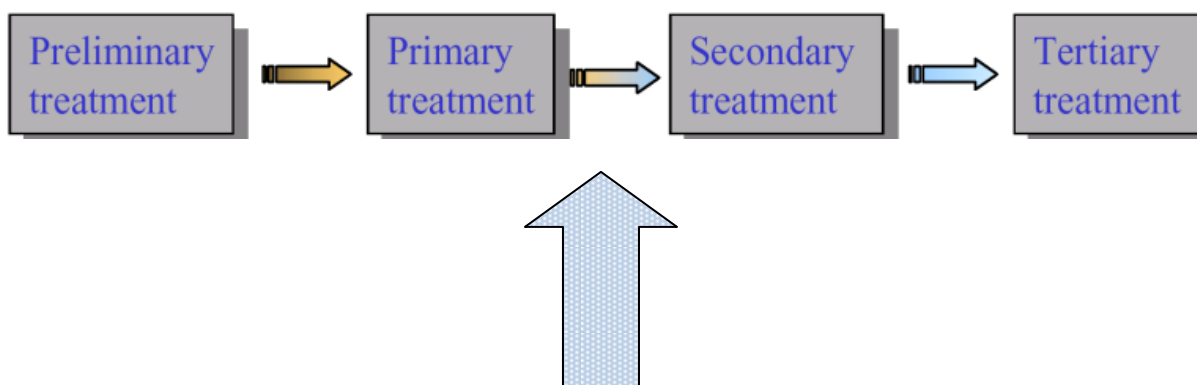
A- N= N- E

A= Aryl/heterocyclic amine component

E = Aryl/heterocyclic or acyclic end coupling component (1)

#### 1.2 Advanced Oxidation Process

In the last decade, a lot of research has been addressed to a particular class of oxidation process called **Advanced Oxidation Process (AOP)**. It has been shown that AOP could be highly efficient to mineralize non-biodegradable molecules into relatively non-toxic inorganic ions and further into CO<sub>2</sub>, H<sub>2</sub>O and mineral acids at ambient temperature and atmospheric pressure. This process could considerably reduce the toxicity of the effluent making it easier for the mills to meet the imposed requirements. One of its drawbacks is its relatively high operational cost. However, this process could come as a pretreatment before the secondary stage (**Fig. 1.1**), therefore solving the problem of the loss of efficiency of the secondary treatment and be economically viable [5].



# AOP

**Fig.1.1.** Schematic representation of wastewater treatment [6]

It is possible to classify the different AOPs. The first parameter is the reaction phase. Indeed either only wet chemical are used, leading to a homogeneous medium or a catalyst in a solid form is used leading to a heterogeneous medium. The second parameter is the nature of the external energy and the third is the way the  $\text{OH}\bullet$  (hydroxyl radical) are produced. The strong potential for water purification of the photo catalytic process is widely recognized but due to high energy cost as is the generation of free hydroxyl radical ( $\text{OH}\bullet$ ), a highly reactive, non-selective oxidizing agent ( $\text{EH}=2.8 \text{ V}$ ), which can destroy even the recalcitrant pollutants. Hydroxyl radicals are effective in destroying organic chemicals because they are reactive electrophiles (electron preferring) that react rapidly and non selectively with nearly all electron-rich organic compounds exhibit faster rates of oxidation reactions comparing to conventional oxidants such as  $\text{H}_2\text{O}_2$  or  $\text{KMnO}_4$ . Once generated, the hydroxyl radicals can attack organic chemicals by radical addition [Eq. (1)], hydrogen abstraction [Eq. (2)] and electron transfer (Eq. (3)). In the following reactions, R is used to describe the reacting organic compound [7].



The photo-catalytic process is based on the irradiation of a catalyst, usually a semi-conductor that creates electron donor and acceptor sites allowing the formation of a highly oxidizing agent:  $\text{OH}\bullet$ . This powerful reactive species attacks with a relatively high rate of reaction and non-selectively most of the organic molecules [8].

The most commonly accepted theory is the following one( **Fig.1.2**)

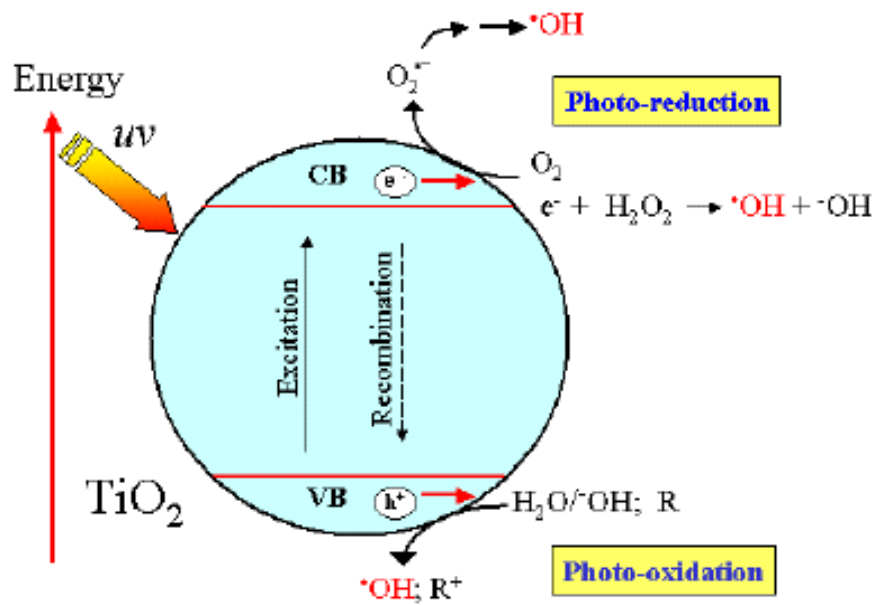


**Fig.1.2.** TiO<sub>2</sub> semiconductor photocatalytic process. Scheme showing some photochemical and photophysical events that might take place on an irradiated semiconductor particle [9]

Heterogeneous advanced oxidation processes generally use catalysts to carry out the degradation of compounds. In comparison to homogeneous processes, such heterogeneous catalysts have the advantage of separating the product with greater ease. For industrial applications, these catalysts should have certain characteristics such as: (1) high activity; (2) resistance to poisoning and long-term stability at high temperatures; (3) mechanical stability and resistance to attrition; (4) non-selectivity in most cases; and (5) physical and chemical stability under a wide range of conditions. Catalysts can be classified as metal catalysts, metal oxide catalysts and organo- metal catalyst. Heterogeneous photocatalysis is the type of heterogeneous AOPs most commonly used these days.

The kinetic for this kind has been studied and follows Langmuir and Freundlich isotherms.

The equation corresponding to the pseudo-first order kinetic model is the following:

$$\log \frac{q_e}{q_e - q_t} = \frac{k_1}{2.303} t \quad (4)$$

where  $q_e$  and  $q_t$  refer to the amount of dye adsorbed (mg/g) at equilibrium and at any time,  $t$  (min), respectively, and  $k_1$  is the equilibrium rate constant of the pseudo-first sorption (1/min). Eq. (5) can be arranged to obtain a linear form

$$\log (q_e - q_t) = \log q_e - \frac{k_1}{2.303} t \quad (5)$$

The equation corresponding to the pseudo-second-order kinetic model is the following

$$\frac{1}{q_e - q_t} = \frac{1}{q_e} + k_2 t \quad (6)$$

where  $k_2$  is the equilibrium rate constant of the pseudo-second-order adsorption (g/mg/min).

Eq. (6) can be arranged to obtain linear form:

$$\frac{t}{q_t} = \frac{1}{k_2 q_e^2} + \frac{1}{q_e} t \quad (7)$$

The theoretical Langmuir isotherm equation can be represented as

$$q_e = \frac{q_{mon} K_L C_e}{1 + K_L C_e} \quad (8)$$

where  $K_L$  is the Langmuir constant related to the energy of adsorption (l/mg) and  $q_{mon}$  is the maximum amount of adsorption corresponding to complete monolayer coverage on the surface (mg/g). The constants  $K_L$  and  $q_{mon}$  can be determined from the following linearised form

$$\frac{C_e}{q_e} = \frac{C_e}{q_{mon}} + \frac{1}{K_L q_{mon}} \quad (9)$$

The essential features of Langmuir adsorption isotherm can be expressed in terms of a dimensionless constant called the separation factor or equilibrium parameter ( $R_L$ ). Conformation of the experimental data into Langmuir isotherm model indicates the homogeneous nature of the catalyst surface.

$$R_L = \frac{1}{1 + K_L C_0} \quad (10)$$

The Freundlich isotherm can be used for non-ideal sorption that involves heterogeneous surface energy systems and is expressed by the following equation:

$$q_e = K_F C_e^{1/n} \quad (11)$$

Where  $K_F$  is a rough indicator of the adsorption capacity and  $1/n$  is the adsorption intensity. In general, as the  $K_F$  value increases the adsorption capacity of an adsorbent for a given adsorbate increases. Eq. (11) may be linearised by taking logarithms:

$$\log q_e = \log K_F + \frac{1}{n} \log C_e \quad (12)$$

Conformation of the experimental data into Freundlich isotherm indicates the heterogeneous nature of the TiO<sub>2</sub> surface.

The processes of degradation for heterogeneous photocatalysis include (i) mass transfer (from the medium to the catalyst), (ii) diffusion, (iii) adsorption, (iv) competition at the surface of the catalyst between the different species, (v) the mechanistic events that take place before any reaction to produce electron-hole pairs from the energy provided by the light.

The photocatalytic degradation of organic pollutants in water generally follows a Langmuir–Hinshelwood mechanism [10] with the rate being proportional to the coverage  $\theta$

$$r = -\frac{dC}{dt} = k\theta = k\frac{K_{ads}C}{1+K_{ads}C} \quad (13)$$

where  $k$  is the true rate constant which is dependent upon various parameters such as the mass of catalyst, the flux of efficient photons, the coverage in oxygen, etc.,  $K_{ads}$  the adsorption constant,  $t$  the time and  $C$  is the concentration of organic pollutant. The product of  $K_{ads}$  and initial concentration cannot be neglected with respect to 1 in the denominator of  $r$  at higher concentrations. Eq. (13) can be rearranged as

$$\frac{1}{k_{app}} = \frac{C_0}{k} + \frac{1}{k K_{ads}} \quad (14)$$

The photocatalytic oxidation rate approaches first order:

$$r = -\frac{dC}{dt} = kK_{ads}C = k'C \quad (15)$$

where  $k'$  is the apparent rate constant of the pseudo-first order kinetics. The integral form,  $C=f(t)$  of the rate equation is:

$$-\ln \frac{C}{C_0} = k_{app}t \quad (16)$$

where  $C_0$  is the initial concentration of pollutant

For the study of adsorption thermodynamics, experiment was conducted at 298 K temperature in order to determine standard free energy ( $\Delta G^\circ$ ). The Gibbs free energy of the adsorption process is related to the equilibrium constant by Eq. (17).

$$\Delta G^\circ = -RT \ln K \quad (17)$$

Where  $R$  (8.314 J/mol.K) is the gas constant,  $T$  (K) the absolute temperature and  $K$  (l/g) is the standard thermodynamic equilibrium constant defined by  $q_e/C_e$ .

## **CHAPTER 2**

### **LITERATURE REVIEW**

#### **2.1 Generalities**

New processes are to be developed to better treat effluents coming from polluting industries. It has been found that advanced oxidation process (AOP) is highly efficient to mineralize non-biodegradable molecules into relatively non-toxic inorganic ions and further into CO<sub>2</sub> and water. Different AOPs exist, but the one that seems relatively interesting is a photocatalytic process with TiO<sub>2</sub> as catalyst. It has been reported in numerous articles that the heterogeneous process using TiO<sub>2</sub> as catalyst is efficient to oxidize organic compounds such as chlorinated phenols, dyes and others like pesticides [11]. The versatility of AOPs is also enhanced by the fact that they offer different possible ways for hydroxyl radical production and thus allowing a better compliance with the specific treatment requirements [12].

## 2.2 Heterogeneous photocatalysts

In recent years, applications to environmental cleanup have been one of the most active areas in heterogeneous photocatalysis and it is inspired by the potential application of TiO<sub>2</sub>-based photocatalysts for the total destruction of organic compounds in polluted air and wastewater.

Semiconductor photocatalysts are preferred in photocatalytic treatments of dye waste-water for the following reasons: (i) they are inexpensive; (ii) they contain low to no toxicity; (iii) they exhibit tunable properties that can be modified such as by size reduction, doping, or sensitizers; (iv) they contain an affording facility for a multielectron transfer process; and (v) they are capable of extending their use without substantial loss in photocatalytic activity [13].

Several metal oxides have been reported to be good photocatalysts, namely titanium dioxide (TiO<sub>2</sub>), zinc oxide (ZnO), tungstate (WO<sub>3</sub>), vanadate (VO<sub>4</sub>), molybdate (MoO<sub>4</sub>) and other [14]. The photocatalytic properties of these metal oxides have been studied extensively and results show that they have active potential as photocatalysts in the degradation of dye in wastewater.

Metal oxides photocatalysts such as zinc, vanadium, tungsten, molybdenum, iridium and cerium oxides have been used to treat dye waste water. Some studies showed that these photocatalysts could be as effective or even better than conventional photocatalysts.

Chakrabarti and Dutta [15] showed that ZnO actually exhibits a higher photocatalytic activity than TiO<sub>2</sub> especially when the degradation of industrial effluents occurs at neutral pH. ZnO showed promising results as a photocatalyst for the degradation of azo dyes (Orange II and Direct Yellow 12) and some reactive dyes (Remazol Black B and Remazol Brilliant Blue R

Cruz *et al.* [16] experimentally showed that under UV conditions Tungsten oxide (WO<sub>3</sub>) was also reported to be photocatalytically active and effective for the treatment of dye wastewater. The different morphologies and physical properties of WO<sub>3</sub>, such as the band gap energy and surface area would determine the treatment efficiency.

Hernández *et al.* [17] worked on cerium oxide (CeO<sub>2</sub>) which received attention as a photocatalyst because of its unique properties of stability under illumination and strong absorption for both UV and visible light. Pure nanocrystalline cubic phase CeO<sub>2</sub> can be prepared using cerium nitrate, NH<sub>4</sub>HCO<sub>3</sub> and polyethylene glycol 1000 as raw material, precipitant and dispersant, respectively. Under appropriate conditions, the synthesized

nanocrystalline CeO<sub>2</sub> was able to degrade Acidic Black 10B up to 97% using sunlight irradiation.

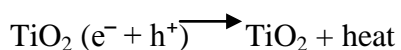
Shang *et al.* 2009 [18] reported that nanosized BiVO<sub>4</sub> with strong visible light induced photocatalytic activity could be synthesized under ultrasonic irradiation using polyethylene glycol (PEG) as a stabilizing agent. They found that the nanosized BiVO<sub>4</sub> exhibited excellent visible light driven photocatalytic efficiency for degrading Rhodamine B; with 1.0 g PEG-modified BiVO<sub>4</sub> fully degrading Rhodamine B in 40 min and reducing the COD content by up to 72.7% in 3.5 h. In contrast, the degradation rate of non-PEG modified BiVO<sub>4</sub> (183 nm) reached 28% after 40 min of visible light irradiation. Thus, the nanosized BiVO<sub>4</sub> by possessing a large surface area, an appropriate band gap and a small crystal size enhances the photocatalytic activity in visible light by up to 12 times higher than catalysts prepared by the traditional solid state reaction.

Ding *et al.* [19] reported a new method of synthesis at a relatively low temperature (lowest temperature 473 K) using solution-combustion of calcium nitrate and indium nitrate as oxidizers and glycine as a fuel, followed by high temperature post annealing (1373 K). Remarkably, this method produced CaIn<sub>2</sub>O<sub>4</sub> rods which showed higher photocatalytic activity for Methylene Blue degradation under visible light irradiation than CaIn<sub>2</sub>O<sub>4</sub> synthesized by the solid state reaction. The CaIn<sub>2</sub>O<sub>4</sub> rods took only 90 min to decompose Methylene Blue under visible light irradiation

TiO<sub>2</sub> is the preferred catalyst for the photocatalytic treatment of dye wastewater. TiO<sub>2</sub> is used as a photocatalyst in dye wastewater treatment mainly because of its ability to generate a high oxidizing electron-hole pair, its good chemical stability, non-toxicity and long-term photostability [20].

### 2.3 Modified TiO<sub>2</sub>

The TiO<sub>2</sub> faces two main problems (a) high energy requirements (photo response). Value of band gap is 3.2eV hence it can absorb wavelength less than 388 nm in UV light spectrum therefore TiO<sub>2</sub> can absorb only 2-3% of solar energies. (b) The main disadvantage of using TiO<sub>2</sub> is the recombination of electrons and holes which can decrease the efficiency of the process.



Modification can be done by incorporating impurities, doping or band gap engineering principles.

Doan *et al.* [21] worked on nano-TiO<sub>2</sub> photocatalysts doped with Iron and Niobium for dye wastewater treatment, which was prepared by temperature-controlled sol-gel method. The effects of these dopants on the physical and chemical properties of TiO<sub>2</sub> were compared with the commercially available Degussa TiO<sub>2</sub> P25. Among these characteristics are crystalline size, the presence of absolute anatase phase, band gap energy and specific surface area. The characterization data were correlated to photocatalytic activities using Turquoise blue dye (TBD) as model pollutant. Single doping (with Nb) and co-doping (Fe and Nb) catalyst reached complete decolorization within 2.5 hours and 3 hours. In addition, their kinetic reaction rate constants of apparent first-order model are 0.0258 min<sup>-1</sup> and 0.0225 min<sup>-1</sup>, respectively.

Bajnoczi *et al.* [22] worked on Fe(III) doped TiO<sub>2</sub> based heterogeneous photocatalysts which were prepared by sol-gel technique( S samples) or flame hydrolysis( F samples). In photocatalytic phenol decomposition, the undoped F samples performed much better, than the undoped S one. However, for the S samples, photocatalytic activity first increased with the increasing Fe(III) concentration, and then passed through a maximum, while Fe(III) doping in F samples significantly decreased it, even at the smallest dopant level.

Song and Yanshan [23] showed that Iron(III) doped TiO<sub>2</sub> powder photocatalysts were prepared by uneven doping using ammonium oleate in order to promote the formation of p-n junction composite structure, and were characterized by X-Ray diffraction, TEM, UV-Vis, PL spectroscopy. The photocatalytic activity of TiO<sub>2</sub> based nanoparticles were evaluated by the photocatalytic rate of methyl orange oxidation. These iron(III) doped TiO<sub>2</sub> photocatalysts are the composite powders having the p-n junction of n-type undoped TiO<sub>2</sub> with p-type TiO<sub>2</sub> doped by Fe evenly, were shown to have a much higher photocatalytic destruction rate than that of undoped TiO<sub>2</sub>.

Yuan *et al.* 2005 [24] studied the photocatalytic activities of brilliant red K2G in solution using Titanium Oxide coated on Activated Carbon(AC) with Fe ions. The results showed that in comparison with agglomeration of pure TiO<sub>2</sub> the TiO<sub>2</sub> particles are well dispersed in AC matrix, of which sizes are decreased with Fe ions doping. Compared with TiO<sub>2</sub>, 0.3% Fe-TiO<sub>2</sub>/AC, 0.5% Fe-TiO<sub>2</sub>/AC and 0.1% Fe-TiO<sub>2</sub>/AC, the 0.3% Fe-TiO<sub>2</sub>/AC showed the highest photocatalytic activity with the complete mineralization of K2G for finite time due to

optimum Fe ions content and AC matrix. Furthermore the kinetic constant ( $k=0.0229 \text{ min}^{-1}$ ) of 0.3% Fe-TiO<sub>2</sub>/AC composite is more than sum of both TiO<sub>2</sub>/AC ( $0.0154 \text{ min}^{-1}$ ) and 0.3% Fe-TiO<sub>2</sub> ( $0.0057 \text{ min}^{-1}$ ).

Costa *et al.* [25] worked on TiO<sub>2</sub> nanotubes which were synthesized in a hydrothermal system. These nanocatalysts were applied to photocatalyse indigo carmine dye degradation. Photodegradation ability of TiO<sub>2</sub> nanotubes was compared to TiO<sub>2</sub> anatase photoactivity. Indigo carmine dye was completely degraded at 60 and 110 min of reaction catalysed by TiO<sub>2</sub> nanotubes and TiO<sub>2</sub> anatase, respectively. TiO<sub>2</sub> nanotubes presented high photodegradation activity at pH 2 and TiO<sub>2</sub> anatase at pH4. TiO<sub>2</sub> nanotubes were easily recycled whereas the reuse of TiO<sub>2</sub> anatase was not effective. Nanotubes maintained 90% of activity after 10 catalytic cycles and TiO<sub>2</sub> anatase presented only 10% of its activity after 10 cycles.

Shrisath *et al.* [26] worked on synthesis of titanium dioxide nanoparticles doped with Fe and Ce using sonochemical approach and its comparison with the conventional doping method. The prepared samples have been characterized using X-ray diffraction (XRD), FTIR, transmission electron microscopy (TEM) and UV-visible spectra (UV-vis). The effectiveness of the synthesized catalyst for the photocatalytic degradation of crystal violet dye has also been investigated considering crystal violet degradation as the model reaction. It has been observed that the catalysts prepared by sonochemical method exhibit higher photocatalytic activity as compared to the catalysts prepared by the conventional methods. Also the Ce doped TiO<sub>2</sub> exhibits maximum photocatalytic activity followed by Fe-doped TiO<sub>2</sub> and the least activity was observed for only TiO<sub>2</sub>. The presence of Fe and Ce in the TiO<sub>2</sub> structure results in a significant absorption shift towards the visible region.

Xueyan *et al.* [27] showed the photocatalytic activity of TiO<sub>2</sub>/heat-treated PVC (HTPVC) film by degrading Rhodamine B (RhB) under visible light irradiation. The photodegradation of RhB follows apparent first-order kinetics. The rate constants of RhB photodegradation in the presence of the TiO<sub>2</sub>/HTPVC films with different mass content of TiO<sub>2</sub> are 16–56 and 4–14 times that obtained in the presence of the pure HTPVC and TiO<sub>2</sub>/polymethyl methacrylate (PMMA) composite film, respectively. The TiO<sub>2</sub>/HTPVC film showed excellent photocatalytic activity and stability after 10 cycles under visible light irradiation.

Guangmei *et al.* [28] showed that TiO<sub>2</sub>- and Ag/TiO<sub>2</sub>-nanotubes (NTs) were synthesized by hydrothermal methods and microwave assisted preparation, respectively. Scanning electron

microscopy, high resolution transmission electron microscopy, Brunauer–Emmett–Teller particle surface area measurement and X-ray diffraction were used to characterize the nanotubes. Rutile TiO<sub>2</sub>-NTs with Na<sub>2</sub>Ti<sub>5</sub>O<sub>11</sub> crystallinity had a length range of 200–400 nm and diameters of 10–20 nm. TiO<sub>2</sub>- and Ag/TiO<sub>2</sub>-NTs with a 0.4% deposition of Ag had high surface areas of 270 and 169 m<sup>2</sup>g<sup>-1</sup>, respectively. The evaluation of photocatalytic activity showed that Ag/TiO<sub>2</sub>-NTs displayed higher photocatalytic activity than pure TiO<sub>2</sub>-NTs and a 60.91% degradation of Rhodamine-B with 0.8% deposition of Ag species. Also 60% of Rhodamine-6G was physisorbed and 40% chemisorbed on the surface of TiO<sub>2</sub>-NTs. In addition, the photocatalytic degradations of organochlorine pesticides taking hexachlorobenzene (BHC) and dicofol as typical examples, were compared using Ag/TiO<sub>2</sub>-NTs, and found that their degradation rates were all higher than those obtained from commercial TiO<sub>2</sub>. Ag/TiO<sub>2</sub>-NTs, and found that their degradation rates were all higher than those obtained from commercial TiO<sub>2</sub>.

Karvinen and Lamminmaki [29] worked on sulfur doped TiO<sub>2</sub> having enhanced activity in the presence of visible light, the production method and use of the same. A sulfur-containing titanium dioxide hydrate precipitate is obtained from an acid titanium oxysulphate solution at a temperature below the boiling point of the solution, e.g. in the range from 70 to 100°C, using crystal nuclei and without addition of base. The precipitate is separated, washed and calcinated. Calcination of the hydrate precipitate is conducted in the temperature range 100 to 500°C, most preferably in the temperature range 200 to 500°C. The catalytic activity has been observed to decrease above and under this calcinations temperature range.

Arai and Saszawa [30] invention is related to TiO<sub>2</sub> doped with molybdenum (Mo). TiO-Mo monocrystalline substance could be obtained by mixing TiO<sub>2</sub> with MoO<sub>3</sub> in the specific proportion, pressure molding the mixture and calcining this in air. The above-mentioned molded body of TiO<sub>2</sub> doped with Mo consists of polycrystalline substance well-regulated in crystal size. In case of the proportion of Mo doped in single crystal is less than 2.0 mol%, the granular growth of crystal is not caused but it is made dense and intercrystalline cracking is not caused. In case the proportion of Mo is more than 8.0 mol%, the granular growth of crystal is irregularly caused and the inter crystalline cracking is not caused.

Hemme *et al.* [31] invention provides pyrogenically prepared titanium dioxide doped by an aerosol and containing, as a doping component, an oxide selected from the group consisting of zinc oxide, platinum oxide, magnesium oxide and/or aluminum oxide as the doping components Hemme *et al.*, 2006) Invented photocatalyst has either: a) a BET surface area of

65 m<sup>2</sup>/g to 80 m<sup>2</sup>/g and a doping component concentration of 40 ppm to 800 ppm, or b) a BET surface area of 35 m<sup>2</sup>/g to 60 m<sup>2</sup>/g and a doping component concentration of more than 1000 ppm.

## CHAPTER 3

### MATERIALS AND METHODS

This section describes the materials as well as the methods used to conduct the experimental work

#### 3.1 Materials

##### 3.1.1 Chemicals and reagents

All chemicals used were of A.R. grade. These were purchased from Sigma-Aldrich chemicals Pvt Ltd. India and SD Fine India.

The chemicals used were 1N HCl and 1N NaOH for adjusting pH, buffer solutions (pH=7 and pH=4) for calibrating pH meter and they were procured from SD Fine, India.

Reactive black 5 dye (55% dye content) was procured from Sigma Aldrich. Reactive black 5 is diazo dye with  $\lambda_{\max}$  597 nm. The structure of RB5 is shown in **Fig. 3.1**.

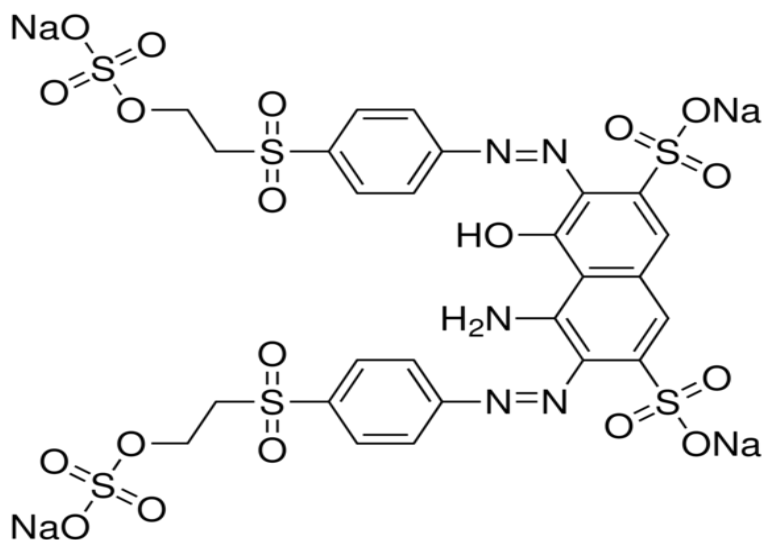


**Fig. 3.1.** Structure of RB5

### **3.1.2 Catalyst**

The catalyst used was Degussa P25 Aeroxide TiO<sub>2</sub> procured from Degussa Company, Germany. Its physiochemical properties are given in **Table 3.1**

**Table 3.1:** Physiochemical properties of Degussa P25 TiO<sub>2</sub>

Physical State	White powder
Composition	80% anatase, 20% rutile
Density(gcm <sup>-3</sup> )	3.8
BET Surface area( m/g <sup>-1</sup> )	55
Average particle size(nm)	30
pH in aqueous solution	3-4

## **3.2 Instruments/Equipment**

### **3.2.1 Radiometer**

UV intensity inside the reactor was measured by Eppley radiometer (model no. 33013)

### **3.2.2 pH meter**

The pH of the solution was measured using ELICO, India, model no. LI 120 pH meter.

### **3.2.3 UV-Vis spectrophotometer**

The concentration of the compounds was determined via spectroscopic analysis. A double beam spectrophotometer from Perkin Elmer, model UV 5704 SS was used.

### 3.2.4 Centrifuge

Samples were centrifuged after treatment in order to separate the TiO<sub>2</sub> particles from the solution. A compact laboratory centrifuge Hitachi High-Speed Micro Centrifuge, Model CF15RX II was used. Samples were centrifuged at a speed of 14,500 RPM until the solution appeared completely free of TiO<sub>2</sub> particles.

### 3.2.5 Photoreactor

The set up comprised of a batch reactor placed on a platform under UV lamps housed in a lamp box (Fig. 3.2 and Fig. 3.3). The lamp box (4'x 2.5' x 2.5') used was made up of galvanized aluminium sheet and fitted with 8 UV black tubes of 40 W each, fitted in parallel on the top of reactor. The UV lamps emit radiation in the range of 300-400 nm, with the peak intensity at 350 nm. UV intensity for all experiments was kept at 10 W/m<sup>2</sup>.

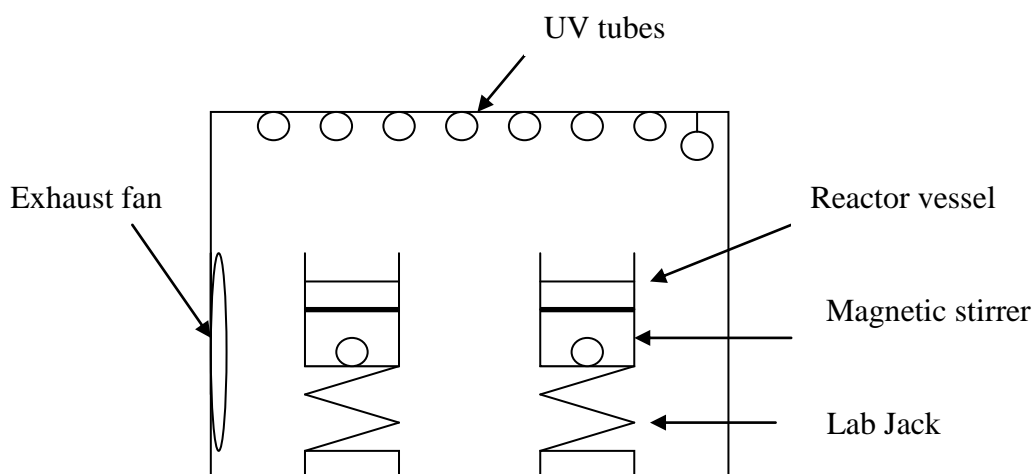


**Fig. 3.2.** Scheme of photocatalytic reactor



**Fig. 3.3** Photocatalytic reactor set up

### **3.3 Experimental Procedure**

#### ***3.3.1 Method for Preparation of TiO<sub>2</sub> Nanotubes***

The titania nanotubes were synthesized by a hydrothermal reaction between NaOH solution and TiO<sub>2</sub>. A total of 20 g of TiO<sub>2</sub> was suspended in 250 ml of 10 mol/l NaOH aqueous solution. This suspension was stirred for 15 min at room temperature and the mixture kept in oven at 150 °C for 72 h. The obtained material was washed with H<sub>2</sub>O and filtered off as shown in **Fig.3.4**. This washed material was suspended in 500 ml, of HCl aqueous solution at pH 2 and stirred for 24 h. HCl treatment was repeated 3 times in order to remove residual sodium ions. After the HCl treatment, the suspension was centrifuged in order to separate the nanocatalyst from suspension [32].

### ***3.3.2 Optimization of parameters***

The parameters like dye concentration, catalyst load, pH were optimized to achieve higher degradation rate.

### ***3.3.3 Adsorption on TiO<sub>2</sub> Suspension***

The adsorption characteristics of RB5 on to TiO<sub>2</sub> (bare and modified) surface were studied by exposing 50 mg/l of dye solution to different amounts of catalyst (0.125g/l-1.75g/l). The dye solution was mixed vigorously in a stirrer with catalyst for 30 minutes. The samples were withdrawn and centrifuged to determine the absorbance at 597 nm to estimate the dye concentration.

### ***3.3.4 Photocatalytic Treatment***

A Borosil circular glass vessel of 500 ml capacity was used as photocatalytic reactor. The area to volume ratio (A/V) of the reactor was kept at 0.202cm<sup>2</sup>/ml for all experiment. This reactor is placed on the lab jack so that required UV intensity could be attained by adjusting the distance of the vessel from the UV tubes. A magnetic stirrer was used to keep the reactor contents well mixed, so that the TiO<sub>2</sub> (bare and modified) stayed suspended. The samples were withdrawn from reactor and centrifuged at 14,500 rpm for 15 minutes to separate catalyst particles.



**Fig.3.4.** TiO<sub>2</sub> nanotubes setup

## **CHAPTER 4**

### **RESULTS AND DISCUSSION**

#### **4.1 Adsorption Mechanism**

The adsorption phenomenon is dependent upon the contact time between the dye solution and adsorbent. In physical adsorption, most of the adsorbate species are adsorbed within short interval of contact time. However, in the case of chemical adsorption, adsorbent requires a longer contact time for the attainment of equilibrium. Adsorption phenomenon is fast during the initial stages and becomes slower near the equilibrium. During the initial stage, large no of active sites are available hence adsorption is more. After certain interval of time, the

remaining vacant surface sites are difficult to be occupied due to repulsive forces between the solute molecules on the solid and bulk phases.

#### 4.1.1 Adsorption Kinetics of Bare TiO<sub>2</sub>

The effect of contact time under different catalyst load on the absorption of RB5 (0.125 g/l - 1.75 g/l) for 50 mg/l dye concentration at pH=4 onto the TiO<sub>2</sub> surface is shown in the **Fig. 4.1**. RB 5 showed faster rate of adsorption during first 5 mins of dye-TiO<sub>2</sub> contact time.

The equilibrium was reached within 10 min. After this equilibrium period, the amount of adsorbed dye did not show time-dependent change.

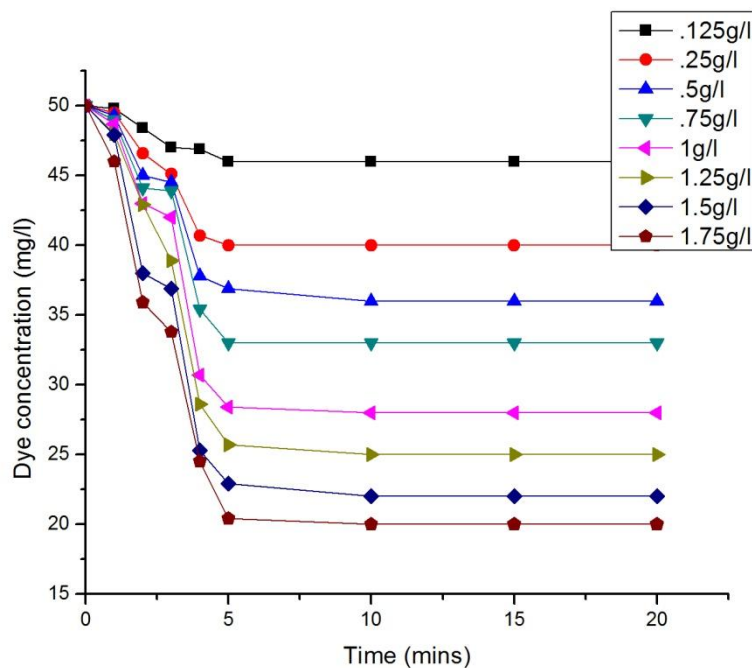


**Fig. 4.1.** Adsorption studies of RB5 on bare TiO<sub>2</sub> (dye conc 50 mg/l, pH 4) at diff catalyst load

**Table 4.1** shows all the adsorption kinetic parameters. The calculated  $q_e$  values for pseudo-first-order model do not agree with the experimental values. The plots of  $t/q_t$  versus  $t$  showed a linear relationship with  $r^2=0.99$  to 1 for pseudo-second-order kinetics model. The calculated  $q_e$  values agree very well with the experimental data and this indicates that the adsorption of dye on TiO<sub>2</sub> surface follows a pseudo-second-order kinetics model.

**Table 4.1.** Adsorption kinetic parameters for different catalyst loadings (0.125 g/l-1.75 g/l) for 50 mg/l dye concentration at pH=4

	First-order kinetic model				Second-order kinetic model		
Catalyst load (g/l)	$q_e(\text{exp.})$ (mg/g)	$k_1(1/\text{min})$	$q_e$ (calculated) (mg/g)	$r^2$	$k_2$ (g/mg.min)	$q_e$ (calculated) (mg/g)	$r^2$
0.125	24.8	0.381	4.8	0.8762	0.007	24.23	0.99
0.25	22.18	0.453	4.31	0.97	0.102	22.20	0.98
0.5	20.87	0.508	3.92	0.92	0.234	20.12	0.99
0.75	19.46	0.563	3.73	.83	0.321	19.76	0.98
1.0	18.76	0.614	3.14	.81	0.49	18.29	.99
1.75	17.14	0.671	2.76	.82	0.5	16.53	0.99

## 4.2 Adsorption Isotherms

Adsorption test was carried in the absence of light to insure that no photocatalytic reaction takes place. The adsorption experiments were conducted with 50 mg/l dye concentration at pH=4 at different catalyst concentrations (0.125 g/l-1.75 g/l). The data were fitted using the Langmuir and Freundlich models. The Langmuir model is applicable to homogeneous adsorption systems when there is no interaction between sorbate molecules, while the Freundlich model is an empirical equation used to describe heterogeneous systems and is not restricted to the formation of the monolayer.

A plot between  $C_e/q_e$  and  $C_e$  is shown in **Fig. 4.3** shows a good fit with  $r^2$  value of 0.9747 and the value of  $K_L$  comes out as 0.108/g. The value of dimensionless separation ( $R_L$ ) Eq 10 is 0.156. The value of  $R_L$  between zero and one indicates the favorable shape of Langmuir isotherm.

The linearized equation that describes the Freundlich isotherm is given by Eq. (12), where  $K_F$  is the adsorption capacity (mg/g) and  $1/n$  is the adsorption intensity (l/g).

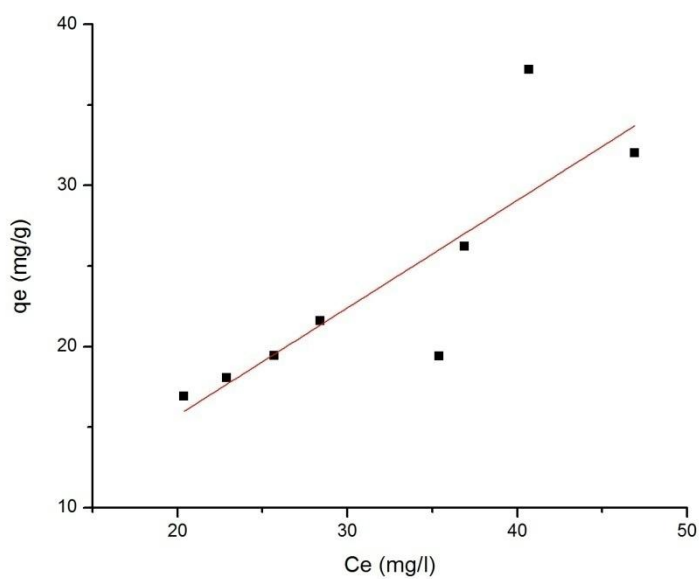


**Fig. 4.2.** Adsorption isotherm of RB 5 onto bare TiO<sub>2</sub> surface (Dye conc. = 50 mg/l, pH=4)

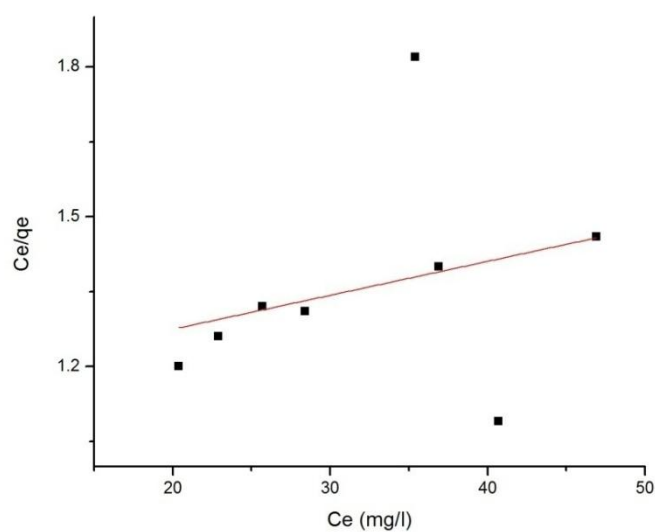


**Fig. 4.3.** Langmuir adsorption isotherm of RB 5 onto bare TiO<sub>2</sub> surface (Dye conc. = 50 mg/l, pH=4)

Through the plot between  $\log q_e$  and  $\log C_e$  (**Fig. 4.4**), the values that fit the experimental data were  $K_F = 4.83$  l/g,  $1/n = 4$  with a correlation coefficient value ( $r^2$ ) = 0.9612

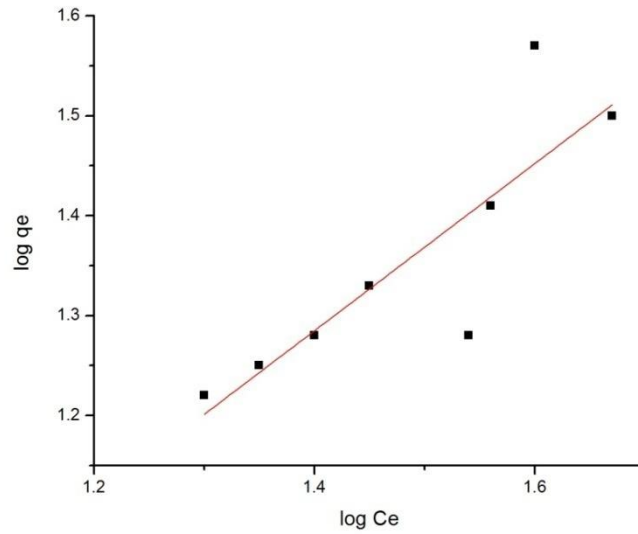


**Fig. 4.4.** Freundlich adsorption isotherm of RB 5 onto bared TiO<sub>2</sub> surface (Dye conc. = 50 mg/l, pH=4)

The  $r^2$  value of both Langmuir and Freundlich isotherms show that both the models are well suited to fit the adsorption isotherm data. **Table 4.2** shows the values of  $q_{\text{mon}}$ ,  $K_L$ ,  $R_L$  for Langmuir isotherms and  $K_F$ ,  $n$  for Freundlich isotherms for reactive black 5.

**Table 4.2:** Langmuir and Freundlich isotherm for adsorption of reactive black 5 on TiO<sub>2</sub> surface (Dye conc. =50 mg/l, pH=4)

Langmuir Isotherm	Reactive black 5	
	$q_{\text{mon}}$ (mg/g)	2.8
	$K_L$ (l/mg)	0.108
	$R_L$	0.156
	$r^2$	0.99
Freundlich Isotherm	$K_F$ (l/g)	4.83
	$N$	4.0
	$r^2$	0.96

### 4.3 Thermodynamic Parameters

The values of  $\Delta G^\circ$  indicate that the adsorption process is non-spontaneous at lower catalyst load (0.125g/l- 0.75 g/l). The value of  $\Delta G^\circ$  is negative for 1.25 g/l and 1.75 g/l catalyst load indicating spontaneous adsorption process at these values of catalyst load as shown in **Table 4.3**.

**Table 4.3** Thermodynamic parameters of the adsorption of RB 5 on TiO<sub>2</sub> surface ( Dye conc. =50mg/l, pH=4)

Cat load (g/l)	K (l/g)	$\Delta G^\circ$ (kJ/ mol)
0.125	0.6823	0.9473
0.5	0.9140	0.2227
0.75	0.7100	0.8484
1.0	0.6101	0.1223
1.5	1.32930	-1.234
1.75	1.46123	-1.942

### 4.4 Photocatalytic Degradation Studies

$$r = -\frac{dC}{dt} = kK_{ads}C = k'C$$

where  $k'$  is the apparent rate constant of the pseudo-first order kinetics. The integral form,  $C=f(t)$  of the rate equation is:

$$\ln \frac{C}{C_0} = -k't$$

where  $C_0$  is the initial concentration of reactive black 5 dye.

**Fig. 4.5** shows the photocatalytic activity of TiO<sub>2</sub>. After adsorption in dark for 30 min (50 mg/l dye concentration, catalyst load 1.7.5 g/l and pH=4) the dye adsorbed was near about 27.5 mg/l. The residual dye concentration in the solution was then irradiated with UV for 6

hr. After photocatalytic treatment for 6 hr, the dye concentration left was 4.32 mg/l i.e. 87 % degradation occurred.

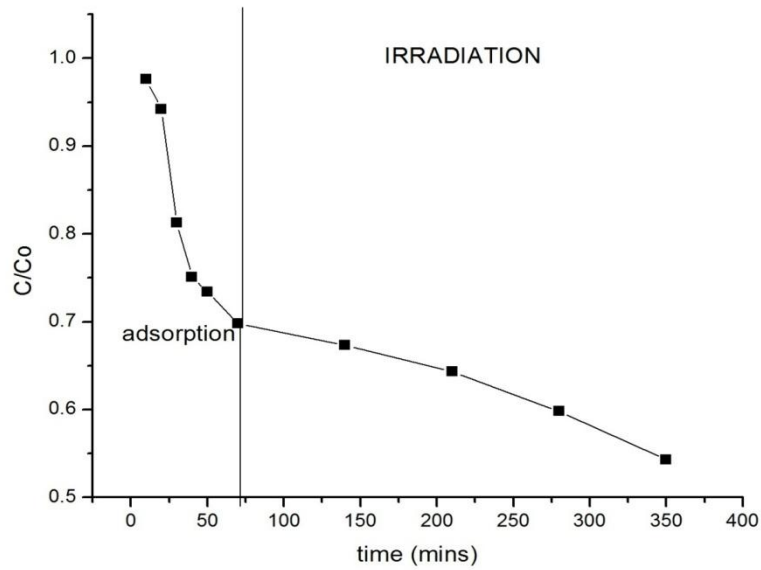


**Fig. 4.5.** Photodegradation of RB5 on bare  $\text{TiO}_2$  surface. (Dye conc. = 50 mg/l, cat load= 1.75 g/l, pH=4).

The value of  $K_{\text{ads}}$  is calculated by plotting graph between  $1/k_{\text{app}}$  and  $C$ . For bared  $\text{TiO}_2$  (**Fig. 4.6**) comes out to be 0.172 l/mg and value of  $k$  is 3.45 mg/l-min. The value of  $K_{\text{ads}}C$  in the denominator cannot be neglected with respect to unity. The photocatalytic oxidation rate approaches first order.

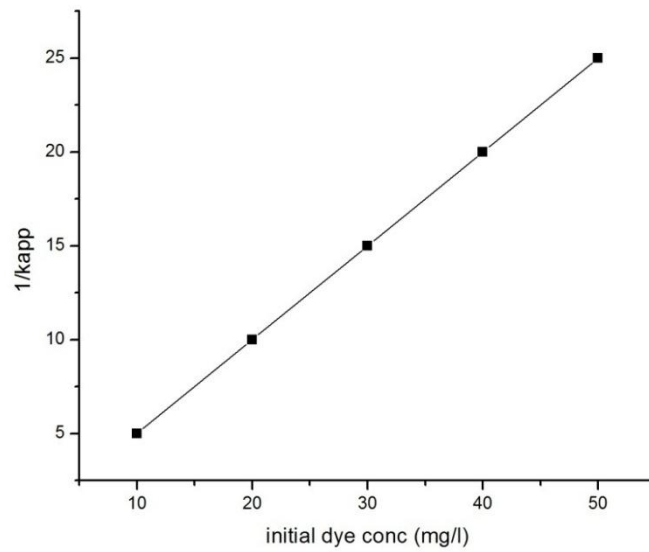


**Fig. 4.6.** Langmuir-Hinshelwood model graph for bare TiO<sub>2</sub>

#### **4.5 Adsorption of dye on TiO<sub>2</sub> nanotubes**

The effect of contact time under different catalyst (TiO<sub>2</sub> nanotubes) loadings on the adsorption of RB5 (0.125 g/l - 1.75.0 g/l) for 50 mg/l dye concentration at pH=2 onto the TiO<sub>2</sub> surface is shown in the **Fig. 4.7**

For TiO<sub>2</sub> nanotubes, the dye solution (50 mg/l) at solution pH=2 did not undergo less adsorption on stirring in the dark for 40 min. The dye absorbed was 29 mg/l.

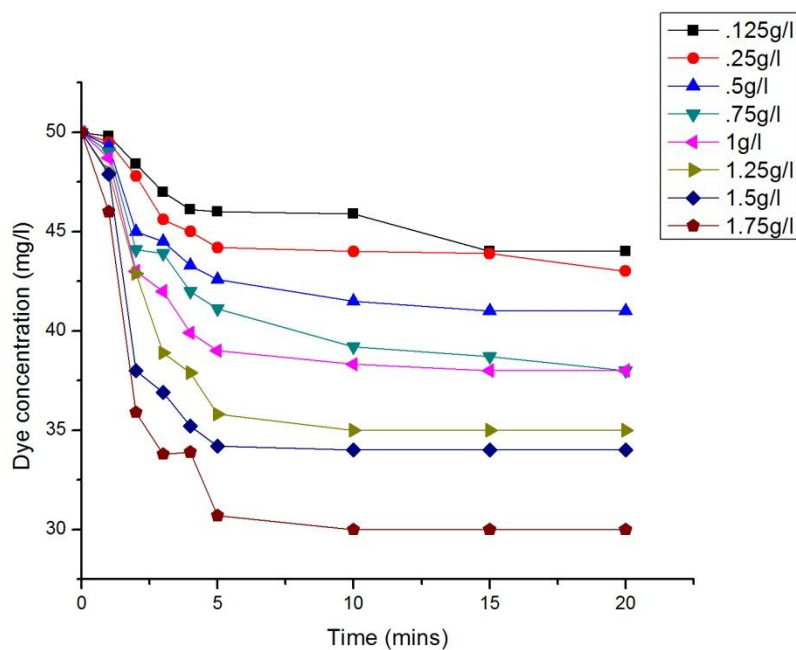


**Fig. 4.7.** Adsorption studies of RB 5 by TiO<sub>2</sub> nanotubes (Dye conc. = 50 mg/l, pH=2)

#### 4.6 Photocatalytic Degradation Studies

For TiO<sub>2</sub> nanotubes the photocatalytic degradation was examined at pH=2 (50 mg/l dye conc, 1.75g/l catalyst load)

**Fig. 4.8** shows the photocatalytic activity of TiO<sub>2</sub> nanotubes. After adsorption in dark for 30 min (50 mg/l dye concentration, catalyst load 1.75 g/l and pH=2) the dye adsorbed was near about 15.32 mg/l. The residual dye concentration in the solution was then irradiated with UV for 6 hr.

After photocatalytic treatment for 6 hr, the dye concentration left was 12.45 mg/l i.e. 65 % degradation occurred.

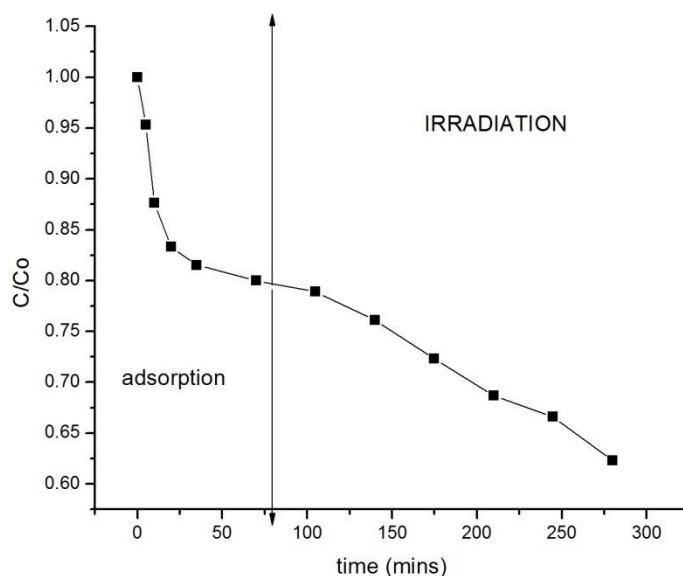


**Fig. 4.8.** Photodegradation of RB5 on TiO<sub>2</sub> nanotubes. (Dye conc. = 50 mg/l, cat load= 1.75 g/l, pH=2).

#### 4.7 Recycling of TiO<sub>2</sub> nanotubes compared with TiO<sub>2</sub> anatase

After reactive black 5 dye photodegradation, the photocatalysts were filtered by simple filtration using a filter paper Whatman and washed with 300ml of water. Then, they were added to a photoreactor to be reused in another reactive black 5 dye solution, in order to perform the same photodegradation.

The recycling studies were followed with TiO<sub>2</sub> anatase and TiO<sub>2</sub> nanotubes in order to compare the catalytic activity, as shown in **Fig 4.9**. The filtration of TiO<sub>2</sub> nanotubes was very quick and easy, whereas the filtration of TiO<sub>2</sub> anatase was very slow and not efficient, due to a loss of approximately 15% of this catalyst during this procedure.

These studies revealed that TiO<sub>2</sub> recovery is difficult and the re-application of these catalysts is not effective. The high stability of TiO<sub>2</sub> anatase in aqueous medium, which generates a high photocatalytic activity, makes its separation from reaction solution difficult.

The activity of TiO<sub>2</sub> anatase decreased dramatically to 10% of dye degradation after 10 catalytic cycles, caused by the material loss during the recovering procedure. On the other hand, TiO<sub>2</sub> nanotubes were easily recycled and maintained 90% of dye degradation after 10 catalytic cycles, showing the TiO<sub>2</sub> nanotubes' ability to be reused in photodegradation reactions.

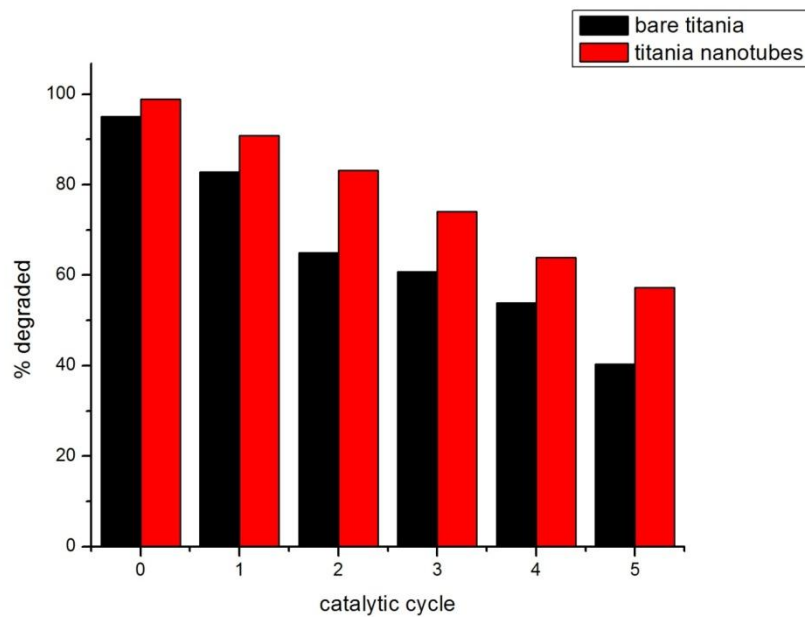


**Fig 4.9**-RB5 degradation for the recycling experiments of the bare TiO<sub>2</sub> and TiO<sub>2</sub> nanotubes

TiO<sub>2</sub> acts faster than TiO<sub>2</sub> nanotubes even if taking into account that nanotubes present a surface area higher than TiO<sub>2</sub>. This fact can be explained by the high stability of TiO<sub>2</sub> suspension in water, which increases the contact between contaminant and catalyst.

#### 4.8 Effect of pH

The degradation was lower in basic medium for both catalysts. The degraded dye amount increases with the reduction of pH value. This behavior can be explained by the decrease of negative charge sites and by the increase of positive charge sites surfaces. In the specific case of TiO<sub>2</sub> anatase, the highest activity was observed at pH 4 and below this value its activity decreased. Below pH 4, the TiO<sub>2</sub> anatase surface is fully protonated. The addition of more

acid in suspension at this pH must cause the increase of proton and chloride concentration, which can collapse the double layer to an extent that the ever-present attractive van der Waals forces overcome the charge repulsion . As a consequence, the decrease of photocatalytic activity was observed in pH below 4 [33].

## **CHAPTER 5**

### **CONCLUSION**

The synthesis of TiO<sub>2</sub> nanotubes is simple and occurred with success. TiO<sub>2</sub> nanotubes presented a photocatalytic activity lower than TiO<sub>2</sub> anatase to degrade RB5 dye. The nanotubes presented the best activity at pH 2 whereas TiO<sub>2</sub> anatase showed its highest activity at pH4. The great advantage of TiO<sub>2</sub> nanotubes in comparison with traditional TiO<sub>2</sub> catalyst is its easy recovery. Consequently, the nanotubes can be recycled and re-applied in many photodegradation cycles, maintaining 90% of their activity after 10 cycles of reaction. The precursor TiO<sub>2</sub> catalyst lost its activity on the second catalytic cycle.

## CHAPTER 6

### RECOMMENDATIONS FOR FUTURE WORK

The future works on photocatalytic treatment could go towards analyzing the effect of other parameters such as: the UV intensity, the influence of O<sub>2</sub>, the influence of metallic ions in the solution, the geometry of the reactor and finally the addition of electron acceptor such as H<sub>2</sub>O<sub>2</sub> without using an univariate method.

It would also be interesting to design an outdoor reactor and implement its installation in India to confirm the possibility of the sun as the source of energy to activate the catalyst in this treatment.

The TiO<sub>2</sub> nanotubes can be doped further to make them more effective.

Finally, an economical study of the process as part of an effluent treatment plant is necessary if one want to enhance such process in the industry.

## REFERENCES

- 1) World Health Organisation, Reducing Risks, Promoting Healthy Life, 2002
- 2) UNESCO (2002). Is the World on Track
- 3) Peavy H.S., Rowe D.R., Tchobanoglous G. (1985). Environmental Engineering, McGraw-Hill
- 4) Anjaneyulu, Y., Chary, N. S., and Raj, D. S. S. (2005). Decolourization of industrial effluents- available methods and emerging technologies. *Rev. Environ. Sci. Biotechnol*, 4, 245–273.
- 5) Anpo M. (2000), In Studies in Surface Science and Catalysis, 130, The 12th International Congress on Catalysis (*Elsevier*), Part A, 157.
- 6) Pozzo R.L., Baltan´as M.A., and Cassano A.E. (1997), Supported titanium dioxide as photocatalyst in water decontamination: state of the art. *Catal Today*, 39, 219–231.
- 7) Ahn, K.Y. and Forbes, L. (2005): US20056884739 .
- 8) Al-Bastaki N.M. (2003). Treatment of synthetic industrial waste-water with UV/TiO<sub>2</sub> and RO using benzene as a model hydrocarbon, *Desalination*, 156, 193.
- 9) Galvez J.B. and Rodríguez S.M. (2003) Solar Detoxification, Edition de 'UNESCO
- 10) Turchi C.S. and Ollis D.F. (1990). Photocatalytic degradation of organic water contaminants: mechanisms involving hydroxyl radical attack. *Catal.* 122 ,178
- 11) Al-Bastaki N.M. (2003). Treatment of synthetic industrial waste-water with UV/TiO<sub>2</sub> and RO using benzene as a model hydrocarbon, *Desalination*, 156, 193.
- 12) Muruganandham M., Swaminathan M. (2007). Solar driven decolorisation of Reactive Yellow 14 by advanced oxidation processes in heterogeneous and homogeneous media, *Dyes and Pigments*, 72, 137
- 13) Chatterjee D. and Dasgupta S. (2005). Visible light induced photocatalytic degradation of organic pollutants. *Photochem Photobiol C – Photochem Rev* 6, 186–205.

- 14) Janitabar-Darzi S. and Mahjoub A.R. (2009). Investigation of phase transformation and photocatalytic properties of sol-gel prepared nanostructured ZnO/TiO<sub>2</sub> composites. *Alloys Compd.*, 486, 805–808.
- 15) Chakrabarti S. and Dutta B.K. (2004). Photocatalytic degradation of model textile dyes in waste-water using ZnO as semiconductor catalyst. *Hazard Mater.*, 112, 269–278.
- 16) Cruz AM-dl, Martínez D.S. and Cuéllar E.L. (2010) Synthesis and characterization of WO<sub>3</sub> nanoparticles prepared by the precipitation method: evaluation of photocatalytic activity under vis-irradiation. *Solid State Sci.*, **12**, 88–94.
- 17) Hernández-Alonso M.D., Fresno F., Suárez S., and Coronado J.M. (2009). Development of alternative photocatalysts to TiO<sub>2</sub>: challenges and opportunities. *Energy Environ Sci*, 2, 1231–1257 .
- 18) Shang M., Wang W., Zhou L., Sun S. and Yin W. (2009). Nanosized BiVO<sub>4</sub> with high visible-light induced photocatalytic activity: ultrasonic assisted synthesis and protective effect of surfactant. *Hazard Mater.*, 172, 338–344
- 19) Ding J., Sun S., Bao J., Luo Z., and Gao C. (2009). Synthesis of CaIn<sub>2</sub>O<sub>4</sub> rods and its photocatalytic performance under visible-light irradiation. *Catal Lett.*, 130, 147–153
- 20) Han .F, Kambala V.S.R., Srinivasan M., Rajarathnam D. and Naidu R. (2009). Tailored titanium dioxide photocatalyst for the degradation of organic dyes in waste-water treatment: a review. *Appl Catal A– Gen.*, 359, 25–40 .
- 21) Doan , Carl Renan Estrellan, Anton Purnomo, Susan Gallardo Chris Salim, Hirofumi Hinode (2012), Characterization and Photocatalytic Activity of Nano-TiO<sub>2</sub> Doped with Iron and Niobium for Turquoise Blue Dye Removal, *AICHE* 2012, Vol. 12, No. 1, 34 – 41.
- 22) Bajnoczia, Nandor Balazsa, Karoly Mogyorosia, David F. Srankoa (2010), The influence of the local structure of Fe(III) on the photocatalytic activity of doped TiO<sub>2</sub> photocatalysts— An EXAFS, XPS and Mossbauer spectroscopic study, *Applied Catalysis B: Environmental* 103 (2010) 232–239.
- 23) Song Liu , Yanshan Chen (2009), Enhanced photocatalytic activity of TiO<sub>2</sub> powders doped by Fe unevenly, *Catalysis Communications* 10 (2009) 894–899.

- 24) MingYuan, Ouyang, YuZhu and Yan WenBin (2005), Preparation of TiO<sub>2</sub>/activated carbon with Fe ions doping photocatalyst and its application to photocatalytic degradation of reactive brilliant red K2G, Science in China Series B: Chemistry.
- 25) Leonardo L. Costa, Alexandre G.S. Prado(2009), TiO<sub>2</sub> nanotubes as a recyclable catalyst for efficient photocatalytic degradation of indigo caramine dye, Journal of Photochemistry and PhotoBiology A: Chemistry-20-45-49.
- 26) S.R. Shirsath , D.V. Pinjari , P.R. Gogate , S.H. Sonawane , A.B. Pandit( 2012), Ultrasound assisted synthesis of doped TiO<sub>2</sub> nano-particles: Characterization and comparison of effectiveness for photocatalytic oxidation of dyestuff effluent, Ultrasonics Sonochemistry .
- 27) Xueyan Li, Desong Wang, Lei Shi(2012), Visible light photocatalytic activity of TiO<sub>2</sub>/heat treated PVC film, J chem. Technol Biotechnol 2012, 87; 1187-1193.
- 28) Guangmei, Binbin Yu, Ping yu(2009), Synthesis and photocatalytic applications of Ag/TiO<sub>2</sub> nanotubes, Talanta 79; 570-575
- 29) Karvinen S., Lamminmaki R.J. (2003): WO03082743.
- 30) Arai, K. and Sasazawa, K. (1998): JP63050324
- 31) Hemme, I., Mangold, H., Geissen, S.U., Moiseev, A. (2006): US20066992042.
- 32) Leonardo L. Costa, Alexandre G.S. Prado(2009), TiO<sub>2</sub> nanotubes as a recyclable catalyst for efficient photocatalytic degradation of indigo caramine dye, Journal of Photochemistry and PhotoBiology A: Chemistry-20-45-49.
- 33) Y.X. Yu, D.S. Xu, Appl. Catal. B 73 (2007) 166–171.

## **PUBLICATIONS**

Mittal V; Bajpai P.K; Bhunia H; Recent Trends in Advanced Oxidation Process for the treatment of dyestuff textile effluent; International Conference on Water Desalination, Treatment and Management(InDAICON 2013),MNIT, Jaipur

